

1 **Lower land use emissions increased net land carbon sink during warming hiatus period**

2 Shilong Piao<sup>1,2,3</sup>, Zhuo Liu<sup>1</sup>, Mengtian Huang<sup>1</sup>, Xuhui Wang<sup>1,4</sup>, Philippe Ciais<sup>4</sup>, Josep G.  
3 Canadell<sup>5</sup>, Kai Wang<sup>1</sup>, Ana Bastos<sup>4</sup>, Pierre Friedlingstein<sup>6</sup>, Richard A. Houghton<sup>7</sup>, Corinne Le  
4 Quéré<sup>8</sup>, Yongwen Liu<sup>1</sup>, Ranga B. Myneni<sup>9</sup>, Shushi Peng<sup>1</sup>, Julia Pongratz<sup>10</sup>, Stephen Sitch<sup>11</sup>,  
5 Tao Yan<sup>1</sup>, Yilong Wang<sup>4</sup>, Tao Wang<sup>2,3</sup>, Zaichun Zhu<sup>1</sup>, Donghai Wu<sup>1</sup>

6

7 <sup>1</sup> Sino-French Institute for Earth System Science, College of Urban and Environmental  
8 Sciences, Peking University, Beijing 100871, China

9 <sup>2</sup> Key Laboratory of Alpine Ecology and Biodiversity, Institute of Tibetan Plateau Research,  
10 Chinese Academy of Sciences, Beijing 100085, China

11 <sup>3</sup> Center for Excellence in Tibetan Earth Science, Chinese Academy of Sciences, Beijing  
12 100085, China

13 <sup>4</sup> Laboratoire des Sciences du Climat et de l'Environnement, CEA CNRS UVSQ,  
14 Gif-sur-Yvette 91191, France

15 <sup>5</sup> Carbon Project, CSIRO Oceans and Atmosphere, Canberra, Australian Capital Territory  
16 2601, Australia

17 <sup>6</sup> College of Engineering, Mathematics and Physical Sciences, University of Exeter, North  
18 Park Road, Exeter EX4 4QF, UK

19 <sup>7</sup> Woods Hole Research Center, 149 Woods Hole Road, Falmouth, Massachusetts 02540, USA

20 <sup>8</sup> Tyndall Centre for Climate Change Research, University of East Anglia, Norwich Research  
21 Park, Norwich, NR4 7TJ, UK

22 <sup>9</sup> Department of Earth and Environment, Boston University, Boston, Massachusetts 02215,  
23 USA

24 <sup>10</sup> Max Planck Institute for Meteorology, Bundesstraße 53, 20146 Hamburg, Germany

25 <sup>11</sup> College of Life and Environmental Sciences, University of Exeter, North Park Road, Exeter

26 EX4 4RJ, UK

27

28

29       **The terrestrial carbon sink has shown an acceleration after 1998, coincident with**  
30 **the warming hiatus<sup>1,2</sup>. However, different mechanisms were proposed<sup>1,2</sup>. Here we analyse**  
31 **recent change in the net land carbon sink (NLS) and its driving factors using**  
32 **atmospheric inversions results<sup>3,4</sup> and terrestrial carbon models. We show that the linear**  
33 **trend of NLS during 1998-2012 ( $0.17\pm 0.05$  PgC yr<sup>-2</sup>) is three times larger than during**  
34 **1980-1998 ( $0.05\pm 0.05$  PgC yr<sup>-2</sup>). This NLS intensification cannot be explained by CO<sub>2</sub>**  
35 **fertilization ( $0.02\pm 0.11$  PgC yr<sup>-2</sup>) and climate change ( $-0.03\pm 0.15$  PgC yr<sup>-2</sup>) according to**  
36 **terrestrial model simulation<sup>5,6</sup>. Thus, we looked more into the contribution of changes in**  
37 **land use emissions (E<sub>LUC</sub>) estimated from the bookkeeping model of Houghton et al.<sup>7</sup>**  
38 **showing decreasing E<sub>LUC</sub> as the dominant driver (73%) of the intensification of NLS**  
39 **during 1998-2012. This reduction of land-use change emissions is due to both decreased**  
40 **tropical forest area loss and increased afforestation in northern temperate regions.**  
41 **Calculating E<sub>LUC</sub> with the inversion-based estimate shows consistently reduced E<sub>LUC</sub>,**  
42 **while another bookkeeping model<sup>8</sup> did not reproduce such change probably due to**  
43 **missing the signal of reduced tropical deforestation. These results highlight the**  
44 **importance of better constraining emissions from land use change to understand recent**  
45 **trends in land carbon sinks.**

46

47 Coincident with the warming hiatus of 1998-2012<sup>9-11</sup>, the vegetation greening trend  
48 observed from several satellite products stalled after 1998 in most regions<sup>12-16</sup> while the global  
49 land carbon sink has continued to increase<sup>1,2</sup>. Keenan et al.<sup>1</sup> and Ballantyne et al.<sup>2</sup> analysed  
50 this signal from the residual terrestrial carbon sink (RLS) calculated by difference between  
51 emissions from fossil fuel and land use, and ocean uptake and atmospheric CO<sub>2</sub> growth rate.  
52 The mechanisms behind the recent increase in RLS were inconsistent between the two studies.  
53 Keenan et al.<sup>1</sup> suggest increasing photosynthesis and decreased respiration, whereas  
54 Ballantyne et al.<sup>2</sup> suggest decreasing photosynthesis and thus reduced respiration being the  
55 only mechanism through which RLS increased during the hiatus. Furthermore, the seasonal  
56 and spatial patterns of changes in land carbon sink do not match with those of temperature  
57 changes<sup>17</sup>. Of note is the fact that systematic errors in land use emissions<sup>7</sup> directly transfer as  
58 bias of RLS<sup>5,18</sup>. Thus, instead of RLS, we revisit changes in the net land carbon sink (NLS)  
59 including land use emissions and its driving factors using atmospheric inversions and land  
60 carbon models.

61 The NLS estimated from the two inversions (see Methods) and from the global CO<sub>2</sub>  
62 budget<sup>19</sup> show a three-times faster increase after 1998 ( $0.17 \pm 0.05$  PgC yr<sup>-2</sup>, mean  $\pm$  1 standard  
63 error) than in the decade before ( $0.05 \pm 0.05$  PgC yr<sup>-2</sup>) (Fig. 1 and Supplementary Table 1, see  
64 Methods). The limit of 1998 is the one used by IPCC<sup>20</sup> and previous carbon cycle study<sup>21</sup> as  
65 the beginning of the hiatus, but using 2001 or 2002 as the starting year of the warming hiatus  
66 yields similar results (Supplementary Table 2). The enlarging positive trend in NLS after 1998  
67 (i.e. NLS intensification) is also found on a 5-years moving window (Supplementary Fig. 1)  
68 and in different inversion versions with more atmospheric CO<sub>2</sub> measurement sites but for  
69 shorter period (Supplementary Table 3 and Fig. 2).

70 NLS can be decomposed as the sum of three components, net primary productivity  
71 (NPP), heterotrophic respiration and fires in natural ecosystems (HR+F) and net carbon

72 emissions from land use change ( $E_{LUC}$ ). The fraction of fire emissions that happens during  
73 land use change, known as deforestation fires, is included in  $E_{LUC}$ , while carbon emission  
74 from fossil fuels for land management is not included in  $E_{LUC}$ . To explain why NLS increased  
75 faster after 1998, we consider three mechanisms: (M1) NPP increased faster than before,  
76 forcing a sink intensification; (M2) heterotrophic respiration and fires (HR+F) increased at a  
77 slower rate than before or declined, consistent with slower warming rates; (M3)  $E_{LUC}$   
78 emissions decreased<sup>22</sup>.

79 **Trends in NPP** For the first mechanism, we analysed NPP changes over the past 30  
80 years using the dynamic vegetation models (DGVM) from the TRENDY project and satellite  
81 observation-based NPP from Smith et al.<sup>12</sup> (hereafter SM16, see Methods). As shown in  
82 Figure 1B and 1D, both satellite-derived NPP and modelled NPP showed significant positive  
83 trends (an indication of enhanced carbon assimilation) before 1998 (SM16:  $0.12 \pm 0.03$  PgC  
84  $\text{yr}^{-2}$ ,  $P < 0.01$ ; DGVMs mean:  $0.15 \pm 0.04$  PgC  $\text{yr}^{-2}$ ,  $P < 0.01$ ). After 1998, however, the  
85 satellite-based NPP shows a significantly ( $P < 0.05$ ) smaller positive trend ( $0.04 \pm 0.04$  PgC  
86  $\text{yr}^{-2}$ ,  $P > 0.05$ ) than before. By comparison, four of the eight DGVMs do not show  
87 deceleration of NPP (i.e. reduced trend of NPP) after 1998, with trend change of NPP ranging  
88 from  $-0.08 \pm 0.05$  PgC  $\text{yr}^{-2}$  ( $P < 0.05$ ) to  $0.11 \pm 0.06$  PgC  $\text{yr}^{-2}$  ( $P < 0.01$ ) (Supplementary Fig. 3).  
89 On average, the DGVMs show almost no change of NPP trend ( $-0.001 \pm 0.067$  PgC  $\text{yr}^{-2}$ ,  $P >$   
90  $0.1$ ) between the period before 1998 and that after 1998 (Fig. 2), and can thus barely explain  
91 ( $< 1\%$ ) the intensification of NLS after 1998. A recent commentary<sup>23</sup> suggested that the  
92 disagreement of NPP trends between SM16 and DGVM is likely due to the underestimate of  
93 the  $\text{CO}_2$  fertilization effect on satellite-based NPP. However, continued increase of  $\text{CO}_2$   
94 concentration over past three decades may not explain the intensification of NLS after 1998.  
95 The leaf area index (LAI) derived from GIMMS satellite products stalled in the recent period  
96 1998-2012, which is not captured by DGVMs (Supplementary Fig. 4). This overestimate of

97 the LAI trend in the period after 1998 suggests that DGVMs may under-estimate the  
98 deceleration of NPP in the recent decade captured in SM16. Therefore, the forcing from NPP  
99 change alone cannot explain why NLS intensified.

100 **Trends in HR and natural fire** To analyse the second mechanism (M2) we analysed  
101 changes in HR based on the same DGVM results<sup>5,6</sup>. As shown in Fig. 2 and Supplementary  
102 Table 1, a reduction in the positive trend of HR (i.e. a deceleration of carbon emission from  
103 HR) in simulations where models were driven by changing CO<sub>2</sub> and climate was found by  
104 most DGVMs, with six out of the eight models showing a reduced trend of HR after 1998  
105 ranging from  $-0.06 \pm 0.03$  PgC yr<sup>-2</sup> ( $P < 0.01$ ) to  $0.06 \pm 0.08$  PgC yr<sup>-2</sup> ( $P > 0.05$ ). The small  
106 deceleration of HR ( $-0.01 \pm 0.04$  PgC yr<sup>-2</sup>,  $P > 0.05$ ), however, accounts for less than 9% (-47%  
107 - 49%) of the observed intensification of NLS. According to factorial DGVM simulations, the  
108 effect of climate change alone (see Methods) did cause a significant deceleration of HR in the  
109 period 1998-2012 ( $-0.04 \pm 0.05$  PgC yr<sup>-1</sup>,  $P > 0.05$ ) compared to the period 1980-1998 (Fig. 2),  
110 consistent with a slower warming rate between 1998 and 2012. However, the climate driven  
111 HR deceleration (i.e. deceleration in carbon emission) is also paralleled by a NPP deceleration  
112 (i.e. deceleration in carbon uptake) due to climate change alone in the DGVM models  
113 ( $-0.06 \pm 0.10$  PgC yr<sup>-2</sup>,  $P > 0.05$ ; Fig. 2). This indicates that the NLS intensification during  
114 1998-2012 cannot be attributed to climate change alone in the DGVM models. The simulation  
115 results of these models further show that rising atmospheric CO<sub>2</sub> can only explain 19% of the  
116 NLS intensification (Fig. 2), and that the combinations of CO<sub>2</sub> and climate change cancel each  
117 other. These results suggest that mechanisms other than CO<sub>2</sub> fertilization and climate change  
118 are responsible for the observed intensification of the NLS.

119 Besides HR, a reduction in natural fire emission could be another cause the  
120 intensification in the NLS. Accounting natural fires at global scale remains challenging,  
121 because satellite-based burn area cannot readily distinguish natural fires from other causes<sup>24,25</sup>.

122 Therefore, we analysed trends in fire simulated by four TRENDYv2 DGVMs, which  
123 considered wild fire processes. The models exhibited large differences in the change of fire  
124 emissions trend during the two periods (CLM4.5:  $-0.052 \pm 0.020$  PgC yr<sup>-1</sup>,  $P < 0.01$ ; LPJ:  
125  $0.004 \pm 0.009$  PgC yr<sup>-1</sup>,  $P > 0.05$ ; VISIT:  $0.007 \pm 0.018$  PgC yr<sup>-1</sup>,  $P > 0.05$ ; LPJ-GUESS:  
126  $0.013 \pm 0.024$  PgC yr<sup>-1</sup>,  $P > 0.05$ ) (Supplementary Fig. 5). However, even considering the full  
127 model range of trend estimates, the natural fire emission probably contributes negatively to  
128 intensification of NLS ( $-6\% \pm 25\%$ ).

129 **Trends in net carbon emission from land use change** Over the last thirty years there  
130 has been a slow-down of forest losses<sup>26-30</sup>. According to the latest Forest Resources  
131 Assessment (FRA 2015) by Food and Agriculture Organization of the United Nations<sup>31</sup>, the  
132 annual rate of net forest loss decreased from 7.27 M ha yr<sup>-1</sup> in the 1990s to 3.99 M ha yr<sup>-1</sup> in  
133 the 2000s, primarily owing to less logging in tropical regions and increased plantations in  
134 northern temperate lands (Supplementary Table 4 and Fig. 6). Therefore, the NLS  
135 intensification can also reflect decreased  $E_{LUC}$  during 1998-2012.

136 We estimated  $E_{LUC}$  using the latest version of the bookkeeping model from Houghton et  
137 al.<sup>7</sup> (hereafter BK), which was widely used and adopted by the Global Carbon Project in  
138 accounting annual global carbon budget<sup>32</sup>. The global  $E_{LUC}$  is a source of 1.13 PgC yr<sup>-1</sup>, which  
139 is found mostly in tropical regions (1.31 PgC yr<sup>-1</sup>), primarily Southeast Asia (0.54 PgC yr<sup>-1</sup>),  
140 South America (0.38 PgC yr<sup>-1</sup>) and Africa (0.38 PgC yr<sup>-1</sup>) (Supplementary Fig. 7a). Tropical  
141 regions are found to be the largest contributor to global  $E_{LUC}$  emissions, followed by the  
142 Southern Hemisphere temperate regions as a slight source (1% of global  $E_{LUC}$ )  
143 (Supplementary Fig. 7a). We then compared the linear trend of  $E_{LUC}$  over the globe between  
144 1980-1998 and 1998-2012. The deceleration of  $E_{LUC}$  contributes to a trend change of  
145  $0.09 \pm 0.01$  PgC yr<sup>-2</sup> ( $P < 0.01$ ) (Fig. 3), explaining 73% of NLS intensification. This result  
146 suggests that the faster increase of NLS after 1998 is primarily explained by decreasing  $E_{LUC}$ .

147 As shown in Fig. 3, the deceleration in global  $E_{LUC}$  between 1980-1998 and 1998-2012 is  
148 attributed to tropical regions, where a decline of  $-0.08 \pm 0.01$  PgC yr<sup>-2</sup> ( $P < 0.01$ ) in  $E_{LUC}$  trend  
149 is found (about 92% of the total decrease in global  $E_{LUC}$  trend). The decline was largely in  
150 Southeast Asia ( $-0.05 \pm 0.01$  PgC yr<sup>-2</sup>,  $P < 0.01$ ) and South America ( $-0.016 \pm 0.004$  PgC yr<sup>-2</sup>,  $P$   
151  $< 0.01$ ) (Fig. 3), where the annual rate of net forest loss declined during the 2000s compared  
152 with 1990s<sup>31</sup>. For example, the rate of net forest loss in South America decreased from 4 M ha  
153 yr<sup>-1</sup> during the 1990s to 3.87 M ha yr<sup>-1</sup> during the 2000s, whereas the net loss rate in Southeast  
154 Asia during the 2000s (0.64 M ha yr<sup>-1</sup>) was only 30% of that during the 1990s (2.11 M ha yr<sup>-1</sup>)  
155 (Supplementary Fig. 6 and Table 4). For NH temperate regions,  $E_{LUC}$  was found to decelerate  
156 between the two periods, with a linear trend of  $-0.010 \pm 0.001$  PgC yr<sup>-2</sup> after 1998 ( $P < 0.01$ ;  
157 about 11% of the total decrease in global  $E_{LUC}$  trend). Temperate North America accounted for  
158 the largest fraction (89%;  $-0.009 \pm 0.006$  PgC yr<sup>-2</sup>,  $P < 0.01$ ) of decreasing  $E_{LUC}$  in the northern  
159 temperate zone, mainly due to the fact that the forest area decrease of  $-0.35$  M ha yr<sup>-1</sup> in the  
160 1990s was reversed to an increase of  $0.22$  M ha yr<sup>-1</sup> after 2000<sup>31</sup> (Supplementary Fig. 6 and  
161 Table 4).

162 In addition to BK based on FAO/FRA land use areas and regional carbon response curves  
163 to land use change<sup>18</sup>, we also explored  $E_{LUC}$  estimates with two other methods, which are the  
164 bookkeeping model of Hansis et al.<sup>8</sup> (hereafter BKH) based on Land Use Harmonization  
165 (LUH) data from 1500 to 2004<sup>33</sup> and the Global Carbon Project update from 2005 to 2012<sup>5</sup>  
166 (see Methods), and  $E_{LUC}$  estimated by forming the difference between the net land-atmosphere  
167 CO<sub>2</sub> flux from atmospheric inversions and the fraction of this flux attributed to natural  
168 ecosystems simulated under the TRENDY S2 DGVM simulation (hereafter  
169  $E_{Inversion-LF-DGVMs(S2)}$ , see Methods). Globally, the change in trend of global  $E_{LUC}$  after 1998 by  
170  $E_{Inversion-LF-DGVMs(S2)}$  ( $-0.07 \pm 0.05$  PgC yr<sup>-2</sup>,  $P < 0.05$ ) was similar to that by BK, but BKH  
171 estimated little change in trend of  $E_{LUC}$  ( $-0.01 \pm 0.01$  PgC yr<sup>-2</sup>,  $P > 0.05$ ) for the same period.

172 The lack of trend change by BKH may come from uncertainties in land cover input dataset.  
173 Important differences between the land use input used in BK, which is directly based on  
174 FAO/FRA, and the harmonized land use dataset by Hurtt et al.<sup>33</sup> used in BKH are assumptions  
175 on shifting cultivation in the tropics and additional assumptions introduced in the latter dataset  
176 to make the country-level FAO/FRA data spatially explicit. Forest cover changes are not  
177 explicitly indicated by the harmonized land use dataset but deduced from changes in  
178 agricultural areas and thus can differ largely from forest inventory data both in magnitude and  
179 in trends (Supplementary Fig. 8). For example, The BKH estimated  $E_{LUC}$  over South America  
180 exhibited positive change ( $0.007 \pm 0.008 \text{ PgC yr}^{-2}$ ,  $P > 0.05$ ) during the warming hiatus period,  
181 which is in contrast to forest survey data suggesting a reduced rate of deforestation in 2000s<sup>31</sup>.  
182 The shift of land cover dataset in 2004 is also a potential issue making BKH more uncertain in  
183 estimating change in  $E_{LUC}$  trend during the recent decade. The general consensus between BK  
184 and  $E_{\text{Inversion-LF-DGVMs}(S2)}$  in estimating change of  $E_{LUC}$  trend globally and over South America  
185 suggests the potential of utilizing this new method in estimating  $E_{LUC}$ . However, it also differs  
186 from BK in estimating trend change of  $E_{LUC}$  at regional scale, for example, over Africa  
187 ( $-0.002 \pm 0.001 \text{ PgC yr}^{-2}$ ,  $P < 0.05$  by BK vs.  $0.04 \pm 0.03 \text{ PgC yr}^{-2}$ ,  $P < 0.05$  by  
188  $E_{\text{Inversion-LF-DGVMs}(S2)}$ ; Supplementary Fig. 7b). The lack of atmospheric CO<sub>2</sub> observations over  
189 Africa can be a large source of uncertainties in atmospheric inversion, as indicated by the  
190 large error bars in regional  $E_{LUC}$  estimates (Supplementary Fig. 7b). The uncertainties in land  
191 carbon models<sup>6</sup> are also propagated in  $E_{\text{Inversion-LF-DGVMs}(S2)}$ .

192 In summary, our results confirm an intensification in the NLS during the warming hiatus,  
193 (1998-2012) as compared to the preceding period (1980-1998). Using different approaches,  
194 we found that a number of drivers were responsible for the enhanced rate of the NLS. The  
195 decreasing trend in net carbon emissions from land use change was the dominant cause during  
196 warming hiatus period. The decreasing emissions from land use change were not driven by a

197 lower rate of warming during this period, but by reduced deforestation in the tropics and  
198 increased afforestation in NH temperate regions. Consistent with Keenan et al.<sup>1</sup>, we found a  
199 lower positive trend of HR due to a lower rate of warming during the second period. But  
200 contrary to them, our analysis, based on an ensemble of DGVMs under different scenarios  
201 instead of a semi-empirical model<sup>1</sup>, shows little effect of HR trends on the NLS, mainly  
202 because of the compensating effects of CO<sub>2</sub> fertilization (increasing carbon emissions from  
203 HR through higher input) and climate change (decreasing carbon emissions from HR). Note  
204 that large uncertainties still remain with estimates of carbon flux from land use change and its  
205 trend over the last thirty years, particularly in East Asia, South America, Africa and Europe.  
206 Reducing this uncertainty is a top priority for future work to more accurately predict the future  
207 evolution of the global carbon cycle and its feedback to climate change. To this end, detailed  
208 information on LULCC transitions<sup>28,34</sup> with high spatio-temporal resolution, and on carbon  
209 response functions to these transitions<sup>30,35</sup> is needed. In addition, various forms of land use  
210 management (e.g. wood harvest, shifting cultivation, cropland management, fire management,  
211 peatland drainage) are often inconsistently and incompletely represented in DGVMs<sup>5,18</sup>. A  
212 better characterization of these critical processes is required in future studies.

213

214 **Methods**

215 **Satellite-based NDVI and NPP data.** The Normalized Difference Vegetation Index (NDVI),  
216 which has been widely used to monitor vegetation activity, was obtained from Global  
217 Inventory Modelling and Mapping Studies (GIMMS) third-generation product (NDVI<sub>3g</sub>) at a  
218 resolution of 8 km×8 km from 1982 to 2015<sup>36</sup>.

219 The satellite-derived net primary productivity (NPP) was from MODIS<sup>13</sup> and a recent  
220 study by Smith et al.<sup>12</sup> (SM16). For the latter, NPP was calculated based on MODIS NPP  
221 algorithm<sup>13</sup>, but driven by 30-year (1982-2011) GIMMS fraction of photosynthetically active  
222 radiation (FPAR) and leaf area index (LAI) data<sup>12</sup>. Further details about satellite-derived NPP  
223 data can be found in Smith et al.<sup>12</sup> and Zhao & Running<sup>13</sup>. Note that the MODIS results only  
224 cover the period from 2001 onwards. Therefore, we only included the MODIS results in  
225 Supplementary Fig. 9 to show that the stall of NPP during warming hiatus period is not an  
226 artifact from the only one long-term satellite-derived net primary productivity (NPP) data  
227 from Smith et al.<sup>12</sup>.

228 **Dynamic global vegetation models (DGVMs).** An ensemble of eight dynamic global  
229 vegetation models (Supplementary Table 5 from the project “Trends and drivers of the  
230 regional scale sources and sinks of carbon dioxide” (TRENDY) were used to simulate the  
231 carbon balance of terrestrial ecosystems during the period 1980-2012. These models provided  
232 outputs of Net Biome Productivity (NBP), Net Primary Productivity (NPP) and Heterotrophic  
233 Respiration (HR). Here we used NBP to reflect the magnitude of net land carbon sink (NLS,  
234  $NLS = NBP = NPP - HR - D$ , D refers to other losses of carbon due to disturbance, including  
235 carbon emissions from land use change). Note that we adopted the convention that a sink of  
236 CO<sub>2</sub> is defined as positive (removing CO<sub>2</sub> from the atmosphere).

237 The DGVMs were coordinated to perform three simulations (S1, S2 and S3) following  
238 the TRENDY protocol<sup>6</sup>. In simulation S1, only atmospheric CO<sub>2</sub> concentration was varied. In

239 simulation S2, atmospheric CO<sub>2</sub> and climate were varied. In simulation S3, atmospheric CO<sub>2</sub>,  
240 climate and land use were varied. The effects of rising atmospheric CO<sub>2</sub>, climate change and  
241 land use change on NLS can then be obtained from S1, the difference between S2 and S1, and  
242 the difference between S3 and S2, respectively. All models used the same forcing datasets, of  
243 which global atmospheric CO<sub>2</sub> concentration was from the combination of ice core records  
244 and atmospheric observations<sup>37</sup>; historical climate fields were from CRU-NCEP dataset  
245 (<http://dods.extra.cea.fr/data/p529viov/cruncep/>); land use data were from the Land Use  
246 Harmonization dataset<sup>31</sup> based on the History Database of the Global Environment (HYDE)<sup>38</sup>.  
247 All the model outputs were resampled to a spatial resolution of 0.5°×0.5° based on the nearest  
248 neighbour method.

249 Note that there is a large difference between TRENDYv2 and TRENDYv4 in the estimate  
250 of NLS trend before and after 1998 under S3 simulation (Supplementary Fig. 10). On average,  
251 NLS in TRENDYv2 shows a non-significant trend before 1998 and a significant increasing  
252 trend after 1998 (Supplementary Fig. 10h), which is consistent with the results from the global  
253 carbon budget and atmospheric inversions. However, in TRENDYv4, an opposite case was  
254 found (Supplementary Fig. 10h). This difference between TRENDYv2 and TRENDYv4 in  
255 simulating the observed NLS trend mainly results from the simulation of land use change  
256 rather than S2 simulation (Supplementary Fig. 10h). This not only indicates large uncertainties  
257 in the simulation of land use change (Supplementary Fig. 7), but suggests the potential effect  
258 of land use change on NLS trend. Although TRENDYv4 used an updated and improved input  
259 of land use change maps (HYDE3.2)<sup>39</sup> compared with TRENDYv2 (HYDE3.1), we did not  
260 adopt it to estimate carbon emissions from land use change given that it did not capture the  
261 trend of NLS before and after 1998. Overall, we only used TRENDY results derived from S1  
262 and S2 simulation in our main text, and proposed a new way to estimate land use change  
263 emission by combining the results from atmospheric inversions and TRENDY models under

264 S2 simulation (see below).

265 **Global carbon budget.** To gain a better understanding of the net land carbon sink, we also  
266 used data from global carbon budget coordinated by the Global Carbon Project (GCP)<sup>19</sup>. Here  
267 the net land sink was inferred as a residual of fossil fuel emissions, atmospheric CO<sub>2</sub>  
268 accumulation and ocean sink, which is independent from atmospheric inversions.

269 **Atmospheric CO<sub>2</sub> inversion data.** Atmospheric CO<sub>2</sub> inversions offer a method in which CO<sub>2</sub>  
270 observation networks, transport models and a prior knowledge of fluxes are utilized to  
271 estimate net land-atmosphere carbon exchange<sup>40</sup>. This top-down approach allows us to  
272 compare the magnitude of net land carbon sink (NLS) with that from bottom-up method based  
273 on DGVMs. Given our long-term study period from 1980 to 2012, here we used two inversion  
274 products: MACC\_v15 from Chevallier et al.<sup>3</sup> (hereafter MACC, available time period:  
275 1979-2015) and JENA\_S81\_v3.8 from Rödenbeck et al.<sup>4</sup> (hereafter JENA, available time  
276 period: 1981-2014). The original spatial resolution of MACC and JENA is  
277 1.875°latitude×3.75°longitude and 3.75°latitude×5°longitude, respectively.

278 It should be noted that there are differences between these two inversions in number of  
279 observation sites as constraint, transport models and prior flux information<sup>40</sup>. As  
280 recommended in previous studies<sup>40,41</sup>, a standard fossil fuel and cement production flux (FFC)  
281 should be subtracted from the total posterior fluxes when comparing net land flux from  
282 different CO<sub>2</sub> inversions. This is due to the fact that differences in prior FFC will manifest as  
283 differences in the estimated natural flux<sup>38</sup>. Thus, here we took the fossil fuel flux which is  
284 used in GCP carbon budget as a standard and subtracted it from the total posterior fluxes for  
285 both CO<sub>2</sub> inversions to obtain the “fossil corrected” NLS, although the global fossil fuel  
286 emissions are quite consistent between the two inversions and with the GCP data  
287 (Supplementary Fig. 11). Note that the FFC data used in GCP carbon budget was from the  
288 Carbon Dioxide Information Analysis Center (CDIAC,

289 [http://cdiac.ornl.gov/trends/emis/meth\\_reg.html](http://cdiac.ornl.gov/trends/emis/meth_reg.html)) and energy statistics published by BP  
290 (<http://www.bp.com/en/global/corporate/about-bp.html>).

291 **Net carbon flux from land use change ( $E_{LUC}$ ).** We used the estimates by Houghton et al.<sup>7</sup>  
292 (hereafter BK) for carbon fluxes due to land use change. In this method, ground-based  
293 measurements of carbon density are combined with land cover change data from the Forest  
294 Resource Assessment (FRA) of the Food and Agriculture Organization (FAO) using a  
295 semi-empirical bookkeeping model, in which standard growth and decomposition curves are  
296 used to track changes in carbon pools<sup>18</sup>. Using the estimate by Houghton et al.<sup>7</sup> is consistent  
297 with the global carbon budget estimates provided by the Global Carbon Project<sup>42</sup>, but may  
298 conceal large uncertainties associated with land use change itself as well as LUC-related  
299 carbon fluxes. We therefore include in the supplemental analyses two additional approaches:  
300 The second approach is also a bookkeeping method but from Hansis et al.<sup>8</sup> (hereafter BKH).  
301 Although BKH largely follows the bookkeeping method developed by Houghton et al.<sup>43,44</sup>,  
302 there are key differences between BKH and BK: BKH is spatially explicit at a resolution of  
303  $0.5^{\circ} \times 0.5^{\circ}$ <sup>8</sup>, whereas BK is constructed based on aggregated, non-spatial national and  
304 international statistics<sup>18</sup>; BKH used Land Use Harmonization dataset from 1500 to 2004<sup>31</sup> and  
305 the Global Carbon Project update from 2005 to 2012 as input<sup>8</sup> while BK used FAO/FRA land  
306 use change data<sup>18</sup>; other differences between BKH and BK are the accounting of successive  
307 LULCC events including their interactions in BKH and different assumptions on the  
308 allocation of agricultural land on natural vegetation<sup>8</sup>. Note that the data available now from  
309 Houghton et al.<sup>43,44</sup> and Hansis et al.<sup>8</sup> does not enable us to obtain the quantifiable  
310 uncertainties for trends.

311 Apart from above two bookkeeping approaches, here we developed a new way to  
312 indirectly estimate  $E_{LUC}$  using the difference of land carbon flux from atmospheric inversions,  
313 the flux from lateral transport (LF) and that from DGVMs under S2 simulation (driven by

314 rising CO<sub>2</sub> and climate change, not taking into account LF) (hereafter referred to  
315 E<sub>Inversion-LF-DGVMs(S2)</sub>). This approach was based on the assumption that the effect of changing  
316 atmospheric CO<sub>2</sub> concentration and climate are well modelled by DGVMs so that the  
317 difference between inversion fluxes (including all CO<sub>2</sub> sources and components), lateral  
318 carbon flux and DGVM modelled fluxes under S2 simulation equals the net source from land  
319 use and land management.

320 The processes of lateral carbon transport generally involve (1) the trade of food and  
321 wood products; (2) carbon export from land to ocean by rivers. In terms of the lateral carbon  
322 flux associated with food and wood trade (Supplementary Fig. 12), we first derive the annual  
323 import and export data of food and wood products from FAO statistical databases  
324 (<http://www.fao.org/faostat/en/#data>). Then the food and wood data are converted into dry  
325 biomass and into carbon using specific conversion factors. For food products, we adopted  
326 crop-specific coefficients (including dry matter content of harvested biomass and carbon  
327 content of harvested dry matter, see Supplementary Table 6) following Wolf et al.<sup>45</sup> and Kyle  
328 et al.<sup>46</sup>. For wood products, we adopted an average wood density of 0.5 and 0.45 carbon  
329 concentration in dry biomass following Ciais et al.<sup>47</sup>. In terms of the carbon exported from  
330 ecosystems by rivers, we included dissolved organic carbon (DOC), particulate organic  
331 carbon (POC) and dissolved inorganic carbon (DIC) from 45 major zones (MARCATS:  
332 MARGins and CATchments Segmentation) and 149 sub-units (COSCATs: Coastal  
333 Segmentation and related CATchments)<sup>48,49</sup> (<http://www.biogeomod.net/geomaps/>, see  
334 Supplementary Table 7). Then we aggregated the riverine carbon transport into continental  
335 scale (Supplementary Fig. 13). However, it should be noted that the carbon transport data is  
336 only a rough estimate and lack temporal evolution. Besides, it is unclear whether the exported  
337 carbon by rivers is from old deposits or from current photosynthesis. In addition, time series  
338 of the carbon exports from rivers are not available. Therefore, we did not count this part in the

339 calculation of LF.

340 Note that we obtained eighteen estimates from  $F_{\text{Inversion-LF-DGVMs(S2)}}$  approach, as eight  
341 DGVMs and two atmospheric inversions were considered in the analysis. All datasets from  
342 atmospheric inversions and DGVMs were first regridded into a common  $0.5^\circ \times 0.5^\circ$  grid using  
343 nearest neighbor interpolation method. We also performed the same analyses by regridding all  
344 the datasets into a common  $1^\circ \times 1^\circ$  or  $2^\circ \times 2^\circ$  grid, and found similar results (Supplementary Fig.  
345 14). In addition, given that BK was based on national data and not spatially explicit, we  
346 obtained latitudinal results (the bottom left in Fig. 3) by roughly aggregating northern North  
347 America, Europe and Asian Russia into boreal region, southern North America,  
348 West/Central/South Asia and East Asia to Northern Hemisphere (NH) temperate region, South  
349 America, Africa and Southeast Asia to tropics, and Oceania to Southern Hemisphere (SH)  
350 temperate region.

351 There is a S3 simulation of TRENDY where DGVMs are driven by the land cover  
352 dataset (LUH) in addition to change in climate and atmospheric  $\text{CO}_2$ . Thus, the difference of  
353 S3 and S2 simulations may also represent the model simulated emission of land use change.  
354 However, comparing the difference between S3 and S2 and  $E_{\text{LUC}}$  estimated by the  
355 bookkeeping or inversion-based approach are difficult, because DGVMs do not simulate the  
356 full range of processes related to  $E_{\text{LUC}}$  (not all DGVMs account for example for wood and  
357 crop harvest or shifting cultivation<sup>42</sup>). Further, land use change emissions derived as  
358 difference between S3 and S2 differ in the terms that are included as compared to other  
359 approaches<sup>48</sup>. Most notably, the loss of additional sink capacity is attributed to  $E_{\text{LUC}}$  using S3  
360 minus S2, while it is excluded from  $E_{\text{LUC}}$  derived from bookkeeping models or the  
361 inversion-based approach. Lastly, the input land cover dataset has discontinuity issue in the  
362 recent decade and different models also have different assumption converting LUH dataset  
363 into model-specific land cover inputs, making it less reliable in estimating trend in the recent

364 decade. Therefore, we do not include the difference of S3 and S2 simulation by DGVMs in  
365 this study.

366 **Statistical analysis.** We calculated the trend of NLS, NPP, HR, NDVI and  $E_{LUC}$  during three  
367 study periods (1980-2012, 1980-1998, and 1998-2012) based on Linear Least Square  
368 Regression analysis, in which above five indicators were regarded as dependent variables and  
369 year as independent variable. The slope of the regression was then defined as the trend. The  
370 standard error of linear regression coefficient (slope) was defined as the uncertainty of the  
371 linear trend. Note that for the average trend of different data sources, the uncertainty of its  
372 trend was estimated as the root-mean-square of the standard error of for each data sources  
373 under the assumption that data from different datasets is independent from each other. Based  
374 on this, we obtained the change of above five indicators' trend between the second period  
375 (1998-2012) and the first period (1980-1998). The dividing year 1998 is selected according to  
376 IPCC description of the warming hiatus period<sup>20</sup>. However, the intensification of NLS and  
377 dominant contribution of  $E_{LUC}$  will not change, if trend analyses starts from 2001/2002 after  
378 the El Nino/La Nina events at the end of 20<sup>th</sup> century (Supplementary Table 2). Note that here  
379 changes in the intensity of each component of NLS were indicated by changes in the  
380 magnitude (absolute value) of each term. In this case, a positive trend in NPP / HR, F and  
381  $E_{LUC}$  refers to an increase of carbon assimilation / carbon emission, and vice versa, a negative  
382 trend in NPP / HR, F and  $E_{LUC}$  indicates a decline in carbon assimilation / carbon emission.  
383 The statistics of the change in trend for each flux was estimated using bootstrap analyses<sup>51</sup>.  
384 We first obtained probability distribution of NLS trend before and after 1998 in 500-time  
385 bootstrapping. Then the probability distribution in the change in trend for each flux was  
386 calculated based on the differences of trends among the sampling of the two probability  
387 distributions. For clarification, NLS intensification indicates increase in the trend of NLS after  
388 1998. Similarly, acceleration/deceleration of a flux (NPP, HR, fire and  $E_{LUC}$ ) indicates

389 larger/smaller trend of the flux during 1998-2012 than that during 1980s-1998.

390 **Data availability.** The GIMMS NDVI<sub>3g</sub> datasets are available  
391 at <http://ecocast.arc.nasa.gov/data/pub/gimms/3g.v0/>. The satellite-derived NPP dataset is  
392 available on request from W. K. Smith<sup>12</sup>. The MODIS NPP dataset is available on request  
393 from M. Zhao<sup>13</sup>. Net carbon flux from land use change (E<sub>LUC</sub>) estimated using the  
394 bookkeeping approach is available on request from R. A. Houghton<sup>7</sup> and E. Hansis<sup>8</sup>,  
395 respectively. Model outputs generated by Dynamic Global Vegetation Model (DGVM)  
396 groups are available from Stephen Stich ([s.a.stich@exeter.ac.uk](mailto:s.a.stich@exeter.ac.uk)) or Pierre Friedlingstein  
397 ([p.friedlingstein@exeter.ac.uk](mailto:p.friedlingstein@exeter.ac.uk)) upon request.

398

399

400 **Reference**

- 401 1. Keenan, T. F. *et al.* Recent pause in the growth rate of atmospheric CO<sub>2</sub> due to enhanced  
402 terrestrial carbon uptake. *Nat Commun* **7**, 13428 (2016).
- 403 2. Ballantyne, A. *et al.* Accelerating net terrestrial carbon uptake during the warming hiatus  
404 due to reduced respiration. *Nat. Clim. Change* **7**, 148-152 (2017).
- 405 3. Chevallier, F. *et al.* CO<sub>2</sub> surface fluxes at grid point scale estimated from a global 21 year  
406 reanalysis of atmospheric measurements. *J. Geophys. Res.* **115**, D21307,  
407 doi:10.1029/2010JD013887 (2010).
- 408 4. Rödenbeck, C. Estimating CO<sub>2</sub> sources and sinks from atmospheric mixing ratio  
409 measurements using a global inversion of atmospheric transport, Technical Report 6, Max  
410 Planck Institute for Biogeochemistry, Jena, available at:  
411 [http://www.bgc-jena.mpg.de/uploads/Publications/TechnicalReports/tech\\_report6.pdf](http://www.bgc-jena.mpg.de/uploads/Publications/TechnicalReports/tech_report6.pdf), 2005.
- 412 5. Le Quéré, C. *et al.* Global carbon budget 2013. *Earth Syst. Sci. Data* **6**, 235-263 (2014).
- 413 6. Sitch, S. *et al.* Recent trends and drivers of regional sources and sinks of carbon dioxide.  
414 *Biogeosciences* **12**, 653–679 (2015).
- 415 7. Houghton, R. A. & Nassikas, A. A. Global and regional fluxes of carbon from land use  
416 and land cover change 1850–2015. *Glob. Biogeochem. Cycles* **31**,  
417 doi:10.1002/2016GB005546 (2017).
- 418 8. Hansis, E., Davis, S. J. & Pongratz, J. Relevance of methodological choices for  
419 accounting of land use change carbon fluxes. *Glob. Biogeochem. Cycles* **29**, 1230-1246  
420 (2015).
- 421 9. Easterling, D. R. & Wehner, M. F. Is the climate warming or cooling? *Geophys. Res. Lett.*  
422 **36**, L08706, doi:10.1029/2009GL037810 (2009).

- 423 10. Kaufmann, R. K., Kauppi, H., Mann, M. L. & Stock, J. H. Reconciling anthropogenic  
424 climate change with observed temperature 1998-2008. *Proc. Natl Acad. Sci. USA*. **108**,  
425 11790-11793 (2011).
- 426 11. Cohen, J. L., Furtado, J. C., Barlow, M. & Alexeev, V. A. Asymmetric seasonal  
427 temperature trends. *Geophys. Res. Lett.* **39**, L04705, doi:10.1029/2011GL050582 (2012).
- 428 12. Smith, W. K. *et al.* Large divergence of satellite and Earth system model estimates of  
429 global terrestrial CO<sub>2</sub> fertilization. *Nat. Clim. Change* **6**, 306-310 (2016).
- 430 13. Zhao, M. & Running, S. W. Drought-induced reduction in global terrestrial net primary  
431 production from 2000 through 2009. *Science* **329**, 940-943 (2010).
- 432 14. Jong, R., Verbesselt, J., Schaepman, M. E. & Bruin, S. Trend changes in global greening  
433 and browning: contribution of short-term trends to longer-term change. *Glob. Change Biol.* **18**,  
434 642-655 (2012).
- 435 15. Mohammat, A. *et al.* Drought and spring cooling induced recent decrease in vegetation  
436 growth in Inner Asia. *Agric. For. Meteorol.* **178**: 21-30 (2013).
- 437 16. Kong, D., Zhang, Q., Singh, V. P. & Shi, P. Seasonal vegetation response to climate  
438 change in the Northern Hemisphere (1982–2013). *Glob. Planet. Change* **148**, 1-8 (2017).
- 439 17. Zhu, Z. *et al.* The accelerating land carbon uptake of the 2000s may not be driven  
440 predominantly by the warming hiatus. *Geophys Res Lett.* **45**: 1402-1409 (2018).
- 441 18. Houghton, R. A. *et al.* Carbon emissions from land use and land-cover change.  
442 *Biogeosciences* **9**, 5125-5142 (2012).
- 443 19. Le Quéré, C. *et al.* Global carbon budget 2015. *Earth Syst. Sci. Data* **7**, 349-396 (2015).
- 444 20. Hartmann, D. L. *et al.* Observations: Atmosphere and Surface. in *Climate Change 2013:*  
445 *The Physical Science Basis* (eds Stocker, T. F. *et al.*) 192–194 (Cambridge Univ. Press,  
446 Cambridge, 2013).
- 447 21. Ballantyne, A. *et al.* Accelerating net terrestrial carbon uptake during the warming hiatus

448 due to reduced respiration. *Nature Climate Change* **7**, 148-152 (2017).

449 22. Grassi, G. *et al.* The key role of forests in meeting climate targets requires science for  
450 credible mitigation. *Nat. Clim. Change* **7**, 220-226 (2017).

451 23. De Kauwe, M. G. *et al.* Satellite based estimates underestimate the effect of CO<sub>2</sub>  
452 fertilization on net primary productivity. *Nat. Clim. Change* **6**, 892-893 (2016).

453 24. Giglio, L., Randerson, J. T. & van der Werf, G. R. Analysis of daily, monthly, and annual  
454 burned area using the fourth-generation global fire emissions database (GFED4). *J. Geophys.*  
455 *Res. Biogeosci.* **118**, 317-328 (2013).

456 25. Andela, N. *et al.* A human-driven decline in global burned area. *Science* **356**, 1356-1362  
457 (2017).

458 26. Rudel, T. K. *et al.* Forest transitions: towards a global understanding of land use change.  
459 *Glob Environ Change* **15**, 23-31 (2005).

460 27. Sánchezcuervo, A. M., Aide, T. M., Clark, M. L. & Etter, A. Land Cover Change in  
461 Colombia: Surprising Forest Recovery Trends between 2001 and 2010. *PLoS One* **7**, e43943  
462 (2012).

463 28. Magliocca, N. R. *et al.* Synthesis in land change science: methodological patterns,  
464 challenges, and guidelines. *Reg Environ Change* **15**, 211-226 (2015).

465 29. Chazdon, R. L. *et al.* Carbon sequestration potential of second-growth forest regeneration  
466 in the Latin American tropics. *Sci Adv* **2**, doi: 10.1126/sciadv.1501639 (2016).

467 30. Poorter, L. *et al.* Biomass resilience of Neotropical secondary forests. *Nature* **530**, 211  
468 (2016).

469 31. Food and Agriculture Organization of the United States (FAO). Global Forest Resources  
470 Assessment 2015: How are the world's forests changing?  
471 <http://www.fao.org/forest-resources-assessment/en/> (2015).

472 32. Le Quéré, C. *et al.* Global carbon budget 2014. *Earth Syst Sci Data* **7**, 47-85 (2015).

- 473 33. Hurtt, G. C. *et al.* Harmonization of land-use scenarios for the period 1500-2100: 600  
474 years of global gridded annual land-use transitions, wood harvest, and resulting secondary  
475 lands. *Climatic change* **109**, 117-161 (2011).
- 476 34. Erb, K. H. *et al.* Bias in the attribution of forest carbon sinks. *Nat. Clim. Change* **3**,  
477 854-856 (2013).
- 478 35. Poeplau, C. *et al.* Temporal dynamics of soil organic carbon after land-use change in the  
479 temperate zone-carbon response functions as a model approach. *Glob. Change Biol.* **17**,  
480 2415-2427 (2011).
- 481 36. Tucker, C. J. *et al.* An extended AVHRR 8-km NDVI dataset compatible with MODIS  
482 and SPOT vegetation NDVI data. *Int. J. Remote Sens.* **26**, 4485–4498 (2005).
- 483 37. Keeling, C. D. & Whorf, T. P. Atmospheric carbon dioxide record from Mauna Loa.  
484 Trends: A Compendium of Data on Global Change. Carbon Dioxide Information Analysis  
485 Center, Oak Ridge National Laboratory, Oak Ridge, TN (2005).
- 486 38. Klein Goldewijk, K., Beusen, A., Van Drecht, G. & De Vos, Martine. The HYDE 3.1  
487 spatially explicit database of human-induced global land-use change over the past 12,000  
488 years. *Global Ecol. Biogeogr.* **20**, 73-86 (2011).
- 489 39. Klein Goldewijk, K. A historical land use data set for the Holocene; HYDE 3.2. *EGU*  
490 *General Assembly Conference Abstracts* **18**, 1574 (2016).
- 491 40. Peylin, P. *et al.* Global atmospheric carbon budget: results from an ensemble of  
492 atmospheric CO<sub>2</sub> inversions. *Biogeosciences* **10**, 6699-6720 (2013).
- 493 41. Thompson, R. L. *et al.* Top–down assessment of the Asian carbon budget since the mid  
494 1990s. *Nat. Commun.* **7**, DOI: 10.1038/ncomms10724 (2016).
- 495 42. Le Quéré, C. *et al.* Global carbon budget 2016. *Earth Syst Sci Data* **8**, 605 (2016).
- 496 43. Houghton, R. A. *et al.* Changes in the Carbon Content of Terrestrial Biota and Soils  
497 between 1860 and 1980: A Net Release of CO<sub>2</sub> to the Atmosphere. *Ecological monographs*

- 498 **53**, 235-262 (1983).
- 499 44. Houghton, R. A. Revised estimates of the annual net flux of carbon to the atmosphere  
500 from changes in land use and land management 1850–2000. *Tellus B* **55**, 378-390 (2003).
- 501 45. Wolf, J. *et al.* Biogenic carbon fluxes from global agricultural production and  
502 consumption. *Glob. Biogeochem. Cycles* **29**, 1617-1639 (2015).
- 503 46. Kyle, P. *et al.* GCAM 3.0 agriculture and land use: data sources and methods. Pacific  
504 Northwest National Laboratory. PNNL-21025 (2011).
- 505 47. Ciais, P. *et al.* The impact of lateral carbon fluxes on the European carbon balance.  
506 *Biogeosciences Discuss* **3**, 1529-1559 (2006).
- 507 48. Laruelle, G. G. *et al.* Global multi-scale segmentation of continental and coastal waters  
508 from the watersheds to the continental margins. *Hydrol. Earth Syst. Sc.* **17**, 2029 (2013).
- 509 49. Regnier, P. *et al.* Anthropogenic perturbation of the carbon fluxes from land to ocean.  
510 *Nature Geosci.* **6**, 597-607 (2013).
- 511 50. Pongratz, J., Reick, C. H., Houghton, R. & House, J. Terminology as a key uncertainty in  
512 net land use and land cover change carbon flux estimates. *Earth System Dynamics* **5**, 177  
513 (2014).
- 514 51. Manly B. F. J. Randomization, bootstrap and Monte Carlo methods in biology (CRC  
515 Press, 2006).

516

## 517 **Acknowledgements**

518 This study was supported by the National Natural Science Foundation of China (41530528),  
519 the 111 Project (B14001), and the National Youth Top-notch Talent Support Program in China.  
520 We thank the TRENDY modelling group for providing the model simulation data.

521

## 522 **Author Contributions**

523 S.Piao designed the study. Z.L performed the analysis. S.Piao and Z.L drafted the paper. All  
524 authors contributed to the interpretation of the results and to the text.

525

526 **Author Information**

527 The authors declare no competing financial interests. Correspondence and requests for  
528 materials should be addressed to S.Piao ([slpiao@pku.edu.cn](mailto:slpiao@pku.edu.cn)).

529

530 **Figure legends**

531 **Figure 1 Anomalies and liner trends of global annual net land carbon sink (NLS) (a, c)**  
532 **and net primary productivity (NPP) (b, d).** Our whole study period is from 1980 to 2012,  
533 and we calculated the trends of above variables for three time periods: 1980-2012, 1980-1998  
534 and 1998-2012. In the left panels, positive value refers to a net carbon sink, while negative  
535 value refers to a net carbon source. The shaded area in the left panels indicates data  
536 uncertainty ( $\pm 1\sigma$ ). In the right panel, we denote significant trends ( $P < 0.05$ ) with two asterisk  
537 based on t test. The error bars in the right panels indicate the standard error of linear trend for  
538 each dataset. In panel (d), the range of the data (minimum-maximum range) across different  
539 models is given as colored vertical bars with the solid line showing the average value. Note  
540 that different colors correspond to different sources of data (see Methods), which are noted in  
541 the legends of each panel.

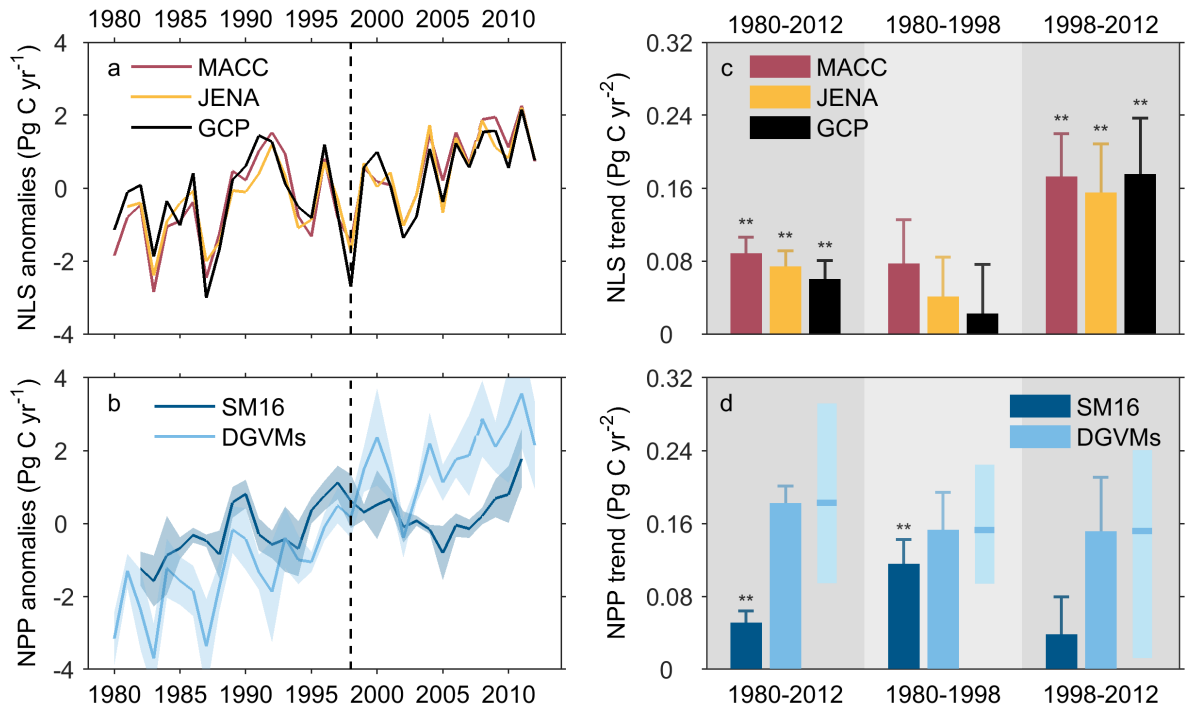
542 **Figure 2 Change in the trend of net land carbon sink (NLS), net primary productivity**  
543 **(NPP) and heterotrophic respiration (HR) estimated by eight Dynamic Global**  
544 **Vegetation Models (DGVMs) under different scenarios between 1998-2012 and**  
545 **1980-1998.** For each model, the change in the trend of NLS / NPP / HR were obtained as the  
546 trend of each variable during 1998-2012 minus that during 1980-1998. Results for the effect  
547 of rising atmospheric CO<sub>2</sub> concentration ('CO<sub>2</sub>'), climate change ('CLI'), and above two  
548 factors combined ('CO<sub>2</sub>+CLI') are shown. On each box, the central line marks the median, the  
549 edges of the box correspond to the 25th and 75th percentiles, and the whiskers extend to the  
550 range of the data. The solid dot shows the average value of the model results.

551 **Figure 3 Linear trend of net carbon emission from land use change (E<sub>LUC</sub>) and change in**  
552 **E<sub>LUC</sub> trend between 1998-2012 and 1980-1998.** The bottom left show results at latitudinal  
553 scale, including boreal (50°N-90°N), northern temperate (23°N-50°N), tropical (23°N-23°S)  
554 and southern temperate region (23°S-60°S). The E<sub>LUC</sub> trend during each of the two periods as

555 well as change in  $E_{LUC}$  trend between two periods are obtained based on annual  $E_{LUC}$  from the  
556 bookkeeping method (BK, see Methods). A positive trend refers to increased  $E_{LUC}$  during  
557 corresponding period, while a negative trend refers to decreased  $E_{LUC}$  during corresponding  
558 period. The error bars indicate the uncertainty for  $E_{LUC}$  trend / the change in  $E_{LUC}$  trend. The  
559 uncertainty of the linear trend was estimated as the standard error of linear regression  
560 coefficient (slope), while the uncertainty of the change in  $E_{LUC}$  trend was estimated using  
561 bootstrap analyses (see Methods).

562

563 **Figure 1**

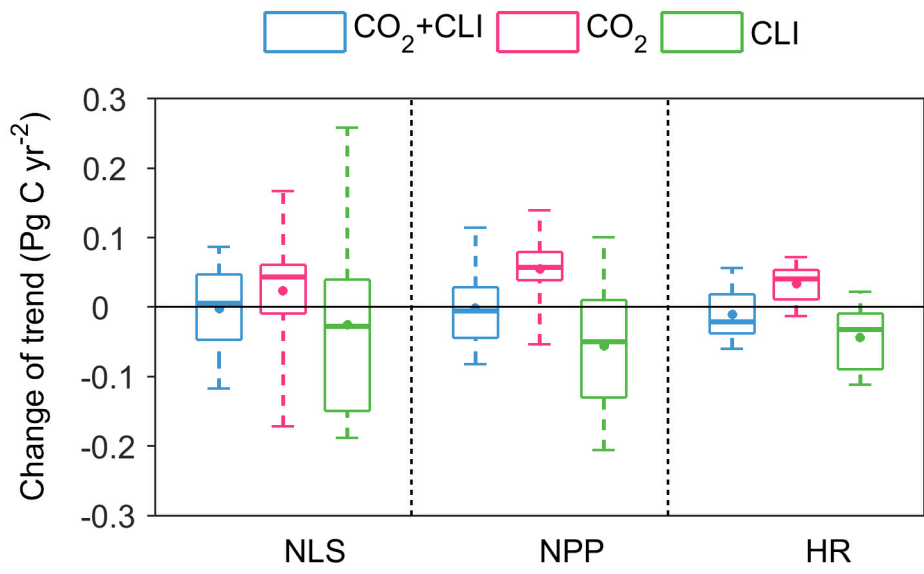


564

565

566

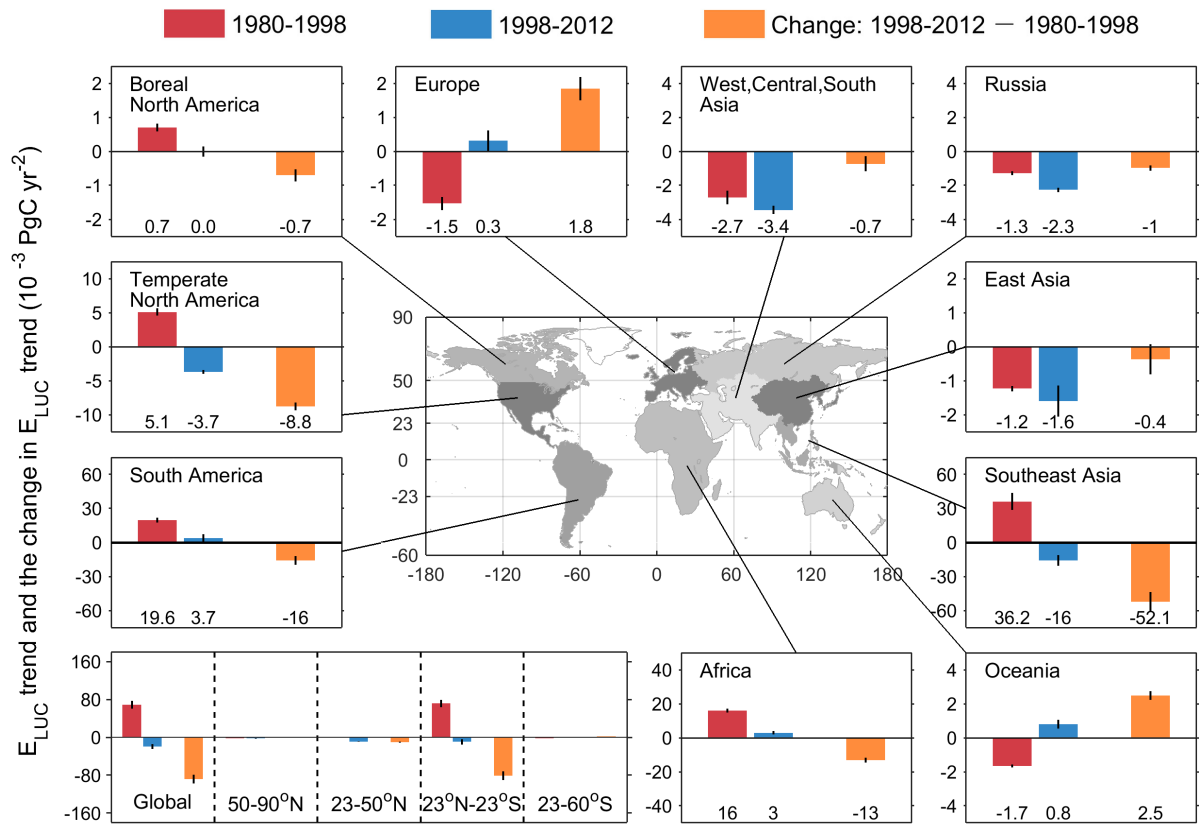
567 **Figure 2**



568

569

570 **Figure 3**



571

572